

**DIGITAL IMAGE CORRELATION APPLICATION IN TENSILE
TEST FOR ALUMINIUM ACCORDING TO
ASTM E-8 STANDARD**

By

Panjaabegesan A/L Ragupathy

Dissertation submitted in partial fulfilment of

the requirements for the

BACHELOR OF ENGINEERING (Hons)

(MECHANICAL ENGINEERING)

SEPTEMBER 2013

Universiti Teknologi PETRONAS

Bandar Seri Iskandar

31750 Tronoh

Perak Darul Ridzuan

CERTIFICATION OF APPROVAL

**DIGITAL IMAGE CORRELATION APPLICATION IN TENSILE TEST FOR
ALUMINIUM ACCORDING TO
ASTM E-8 STANDARD**

By

Panjaabegesan A/L Ragupathy

A project dissertation submitted to the
Mechanical Engineering Programme
Universiti Teknologi PETRONAS
in partial fulfillment of the requirement for the
BACHELOR OF ENGINEERING (Hons)
(MECHANICAL ENGINEERING)

Approved:

Dr. Saravanan Karuppanan

Final Year Project Supervisor

UNIVERSITI TEKNOLOGI PETRONAS

TRONOH, PERAK

December 2013

CERTIFICATE OF ORIGINALITY

This is to certify that I am responsible for the work submitted in this project, that the original work is my own except as specified in the references and acknowledgements, and the original work contained herein have not been undertaken or done by unspecified sources or persons.

PANJAABEGESAN A/L RAGUPATHY

ABSTRACT

Digital image correlation method is a non-contact method for strain measurement. This project was aimed to investigate the use of simple tools to obtain strain values. The objective was to evaluate the suitability of strain measurement method by processing images captured using a digital camera. The tools included an 8 MP digital camera, a 2kN Universal Tensile Machine and Matlab R2009a as the image processing software. An aluminium specimen was loaded in tension according to ASTM E8 testing method while the CANON camcorder captured the video of specimen being loaded. Once the video was captured, the images were snapshot from video strip using a built-in function of the camera. After that, the images were processed using the Mathlab R2009a software. Strain was calculated using the change in length in the y coordinate of the images. The results showed good agreement between experimental and literature values. From the stress-strain curves, the modulus of elasticity of the respective materials was determined and the results determined by the extensometer and the optical strain measurement method were compared to each other. The results had been verified as the modulus of elasticity of the aluminium specimen was 6.99% off the literature values. The findings suggested that the optical method has high potential to be a useful method for strain measurement for various other materials.

ACKNOWLEDGEMENTS

First and foremost, I would like to express my outmost gratitude towards my project supervisor, Dr. Saravanan Karuppanan for taking me under his wing and providing me all the necessary resources, not only to accomplish this project, but also to enrich my character and knowledge further.

I also would like to extend my heartiest appreciation to my fellow mentor, Mr. Khoo Sze Wei who helped and cooperated with me throughout the project. Next, I would like to thank the lab technicians, especially Mr. Paris who provided me with the guidance in completing this project despite many other obligations. Many thanks to my family back home for their sacrifices coupled with their continuous encouragement and support in heading me towards success. Special thanks to all the members of the Mechanical Engineering Department of Universiti Teknologi PETRONAS (UTP), for establishing continuous support and backing me up.

Last but not least, my appreciation is also extended to my friends and everyone who encouraged and supported me throughout the successful completion of this Final Year Project.

	3.3.2	Experimental Set-Up	.	.	23
	3.3.3	Tensile Test Experiment and Video Recording during Strain Inducing Event	.	.	25
3.4		Optical Strain Measurement Method validation with Experimental Results	.	.	26
3.5		Gantt Chart and Key Milestone	.	.	28
3.6		Tools required	.	.	28
CHAPTER 4:		RESULTS AND DISCUSSION	.	.	30
4.1		Validation of Optical Strain Measurement Method with Experimental Results			30
4.2		Comparison to Specimens Material Properties	.	.	33
CHAPTER 5:		CONCLUSIONS AND RECOMMENDATIONS	.	.	37
5.1		Conclusions	.	.	37
5.2		Recommendations	.	.	38
REFERENCES			.	.	40

LIST OF FIGURES

Figure 2.1: Aluminium consumption world wide	8
Figure 3.1: Process flow chart of study	12
Figure 3.2: Final Year Project Flow Chart	13
Figure 3.3: Gray Scale Images from Hovis, 1989	15
Figure 3.4: The speckles coordinates in an image	16
Figure 3.5: The orientation of the line element in PQ in the reference image	17
Figure 3.6: Electrical Discharge Machining Machine	19
Figure 3.7: The cutting process of the EDM machine	20
Figure 3.8: The shape of the aluminium specimen	20
Figure 3.9: The AutoCAD drawing of the dog bone specimen	21
Figure 3.10: The 20kN UTM machine that was used for the tensile test	22
Figure 3.11: The equipment used in the tensile test	23
Figure 3.12: The setting of the specimen before the experiment being conducted	24
Figure 3.13: The result of one of the tensile test specimen.	25
Figure 3.14: Elongation values extracted from the data logger	26
Figure 4.1: The tensile test chart	30
Figure 4.2: Stress strain curve for all five aluminium specimen	31

Figure 4.3: Specimen image taken at 1 second	32
Figure 4.4: Specimen image taken at 44 seconds	33
Figure 4.5: Specimen image taken at 90 seconds	33
Figure 4.6: Specimen image taken at 134 seconds	34
Figure 4.7: Specimen image taken at 178 seconds	34
Figure 4.8: Specimen image taken at 222 seconds	35
Figure 4.9: Specimen image taken at 266 seconds	35
Figure 4.10: Specimen image taken at 310 seconds	36
Figure 4.11: Specimen image taken at 354 seconds	36
Figure 4.12: Specimen image taken at 398 seconds	37
Figure 4.13: Specimen image taken at 482 seconds	37
Figure 4.14: Determination of the modulus of elasticity for the specimen	39
Figure 4.15: Specimen before tensile test	40
Figure 4.16: Four irregular placement of the speckles that will assisted in identification of the speckles during Matlab simulation.					41
Figure 4.17: Final image at $t=360$ seconds which illustrates the hourglass effect where the localized stress have occurred.					42
Figure 4.18: Specimen on the right is the undeformed specimen while the specimen on the left is the deformed specimen.					43

LIST OF TABLES

Table 3.1: Material properties of aluminium	18
Table 3.2: Dimension of the aluminium specimen	21
Table 3.3: Settings for the video camera	24
Table 3.4: Gantt Chart and Key Milestones for FYP I and FYP II	27
Table 4.1: Results obtained from the extensometer for the tensile test experiments	29
Table 4.4: Comparison of the modulus of elasticity determined by the extensometer and the optical strain measurement method	40

CHAPTER 1

INTRODUCTION

1.1 Background of Study

As compared to the traditional extensometer, optical strain measurement method have been increasingly applied in recent years for various materials to characterize their mechanical behavior. In contrast to clip-on or contact extensometers, which are mechanically attached to the test specimen, optical measurement devices operate contactless. Optical techniques are particularly suitable for a wide range of materials, for example, where strength and high modulus are important parameters. This is because in contact measurement system, local stress concentrations arise from the indentation of the specimen. Optical technique avoid this problem. There are two main principles of optical strain measurement system that can be distinguished. One is the commonly known as video extensometers and the other is known as full-field strain analysis (FFSA) or commonly referred to as digital image correlation (DIC) [1]. In general, DIC is based on the principle of comparing speckle pattern structure on the deformed and the undeformed sample or between any two deformation states. For this purpose, black speckles are sprayed on the specimens in a specific manner and these speckles are followed during the deformation by the digital camera system. In this manner, the information of the in-plane local strain distribution is gained. Furthermore, the main benefit of this method is that, it is independent of geometry and can also be applied to different shapes to gain information on the deformation behavior of components in real service [2].

For traditional extensometer, the limits of resolution and accuracy are well known and can easily be determined. It is more complicated in the case of optical measurement system. This is because since resolution and accuracy depends on the whole measurement system. The measurement system includes the specimen, the camera and the lighting system. The most important character of the optical

system is the number of pixels per mm. This is because the pixel per mm value affects the resolution of the optical system mentioned here. All these values depend on the distance between the camera and the specimen. Moreover, out-of-plane movements of the specimen affects the apparent size of the specimen and, thus, may also alter the strain results in 2D measurements.

1.2 Problem Statement

Digital image correlation method is being widely used for displacement measurement in various areas of science and engineering. This method possess many advantages over other optical methods. Some research suggests that DIC has these following advantages:-

- i) Low difficulty in handling
- ii) No localized stress concentration on specimen
- iii) No profound need for very complicated fringe pattern analysis or light waves reconstruction to obtain the strain value

Therefore, there is a need for proof that DIC can actually be used for a wider range of materials, especially focusing on aluminium. This is because aluminium is widely used in everyday application from airplanes to our household knives. A more precise measurement of strain is needed. In this study, a consumer version of high-definition video was used to capture the images during tensile test with the intention of using aluminium as the priority specimen.

1.3 Objectives

The objectives of this project are:

- i) To evaluate the suitability of strain measurement of aluminium by processing images captured using a digital camera

- ii) To compare the results obtained by DIC with those obtained by a conventional mechanical transverse extensometer

1.4 Scope of Study

This project focuses on the analysis of aluminium specimen using the Digital Image Correlation method. The “dog bone” specimen of the aluminium is cut using Electron Discharge Machine for perfect cutting. The main parameters that will be of attention during the study is the strain values. The values, one from the extensometer and the other from the image analysis will be compared to determine the suitability of DIC for aluminium.

1.5 Significance of Study

There is not much written information in this area for aluminium that is related to effect of using DIC in tensile test for aluminium specimen. In this research, the result can be obtained and the strain values be determined by analysis of the images. The accuracy of the data can further be increased with assistance of this project.

CHAPTER 2

LITERATURE REVIEW

2.1 Digital Image Correlation Method

The DIC method has been since the early 1980s and takes a number of different forms. The technique in focus for this study is the 2-dimensional DIC and it involves the use of a single camera to measure the displacements in a plane. This technique has the advantage that it only requires a single camera, thus minimizing the equipment costs and allowing for additional measurement to be added. However, it has one significant disadvantage, which is that all the displacements that occurs must be within the single stationary measurement plane or else major error of results will be generated [3-8].

The DIC method has previously been used by researchers to measure axial strain for artificially and experimentally generated images, with varying degrees of success. Smith *et al.*, 1998 reported a standard deviation in strain reading of 100 $\mu\epsilon$. Though concentric lens was used, which will minimize the effects of out-of-plane distortion, the camera resolution of 640x480 pixels, had negative effect on their measurement accuracy. Displacement errors produced using the DIC technique are generally fractions of a pixel and when measuring strain, the effect of this error can be reduced by using a larger gauge length to produce a lower strain error. Thus higher resolution cameras (which will be used in the current work) enhances measurements accuracy by allowing for larger gauge lengths. Wattrisse *et al.*, 2001 obtained mean strain errors of 210 $\mu\epsilon$, but similar to Smith *et al.*, they used a lower resolution camera (1317 x 1035 pixels) as well as a less accurate sub-pixel interpolation scheme. Additionally, Wattrisse *et al.*, used a lens with a small focal length of 55 mm. The focal length of the lens is an important factor in improving strain measurement error. Larger focal length corresponds to smaller errors.

The DIC method discretizes a digital image into smaller areas known as subsets. The movement of these subsets in a series of digital images is then tracked between subsequent images. The strain resolution that can be measured is a function of the software's ability to track the movement of these subsets with sub-pixel accuracy.

The measurement of displacements and strains has always been an important topic of material properties, such as material strengths or fracture parameters and in experimental stress analysis. Optical techniques such as moiré interferometry, holography, and speckle interferometry have been proven matured techniques to analyze macroscopic parameters and are being applied successfully in many different applications. The processing of fringe patterns is laborious and time consuming. This technical difficulty has raised many researchers attention and computerized procedures have been developed to automate the processing of the data from the fringe patterns.

In the last two decades, Sutton et al., [5] and Bruck, et al., [6] have developed the DIC method. It was applied to measurement of displacements and strains. The applications include microscopic strain measurements in electronic packaging [7] , strain fields in polyurethane foam plastic materials and evaluation of their mechanical properties [11]. This methodology was even used for in situ evaluation of the state of conservation of mural frescoes [13]. This computer vision technique has the advantage of a simple system and direct sensing. The DIC method as explained earlier uses two images, which were captured by a solid-state video camera, to represent the states of the object before and after deformation. Both of the digitized images were then correlated by an algorithm, based on mutual correlation coefficient or other statistical functions to find out the subtle differences in them.

The core of digital image correlation in this application depends on the ability to recognize two nearly similar, yet different, image patterns. *Bruck et al.*, [4] mentioned in his study the Newton-Raphson method. It was used and showed that the computation of

correlation has been drastically decreased in comparison with the course-fine search algorithm. The methodology used by Newton-Raphson assumed that the local deformation is uniform and therefore the local deformation could be represented by two displacements and four displacements gradients, commonly known as strains. This was used as a basis for speckle pattern that would be used in this experiment.

2.2 Tensile Test

Tensile test are performed for several reasons. The results of tensile test are used in selecting materials for engineering applications. Tensile properties frequently are included in material specifications to ensure quality. Tensile properties often are measured during development of new materials and processes, so that different materials and process can be compared. Finally, tensile properties often are used to predict the behavior of a material under different forms of loading other than uniaxial tension. The strength of a material is often the primary concern. The strength of interest maybe measured in terms of either the stress necessary to cause appreciable plastic deformation or the maximum stress that the material can withstand. These measures of strength are used, with appropriate caution in the form of safety factors in engineering design [9-11].

2.2.1 Universal Testing Machine

Most studies of ductility have concentrated on the specimen geometry and the influence of machine design, grips, alignment and other may often be taken for granted. Machine control and frame stiffness can also have a profound effect on ductility, particularly in the case of reduction in area measurements, as the final necking and fracture phase of a test is characterized by instability. A machine with stiff frame and a rapid strain rate control response will be capable of unloading the specimen in a progressive manner to inhibit the onset of instability and may therefore achieve greater

reduction in area of the specimen and a higher measured elongation. Markowski [12] designed used a special research machine with a very stiff inner frame, which did not unload energy in an uncontrolled manner into a test piece. Thus from here it was inferred that ductility is not an absolute inherent material property since it is highly dependent upon the testing machine, the testing conditions and the form of the test piece.

2.3 ASTM E8 Standard

Tensile testing requirements are specified in various standards for a wide variety of different materials and products. The standard that is mainly followed for the experiment is American Society of Testing and Material (ASTM) E-8, which is for Standard Test Method for Tension Testing of Metallic Materials. These specifications define the requirements for the test apparatus, test specimens, and test procedures.

Standard tensile test are conducted using a threaded tensile specimen geometry of ASTM E 8. For thin plate or sheet materials, a flat, or dog-bone specimen geometry is used. The dog bone specimen is held in place by wedge shaped grips. The holding capacity of the grips provides a practical limit to the strength of material that a machine can test.

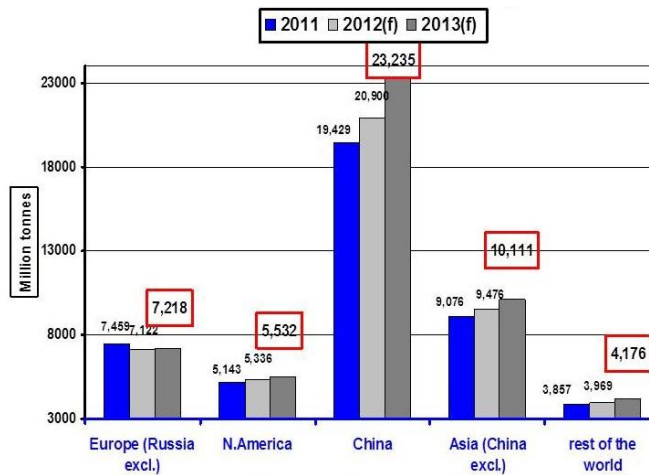
Accuracy and precision of test results can only be quantified when known quantities are measured. Materials with unknown properties cannot be used because there are not any reference data for the material. This allows the comparison of material's properties with known properties as reference material. Test of standard material would reveal the system accuracy and repeated experiments would quantify its precision and repeatability. A variety of factors influences accuracy, such as precision and repeatability of test results. Errors can be grouped into three broad categories:-

- Instrumental errors: these can involve machine stiffness, accuracy and resolution of the load cell output, alignment of the specimen, gripping of the specimen, and accuracy of the extensometer.

- Testing errors: these can involve initial measurement of specimen geometry, electronic zeroing and establishing a preload stress in the specimen.
- Material factors: these describe the relationship between the material intended to be studied and that being tested. Other material factors would include specimen preparation, specimen geometry and material strain rate sensitivity.

2.4 Testing Material

Figure 2.1 shows the primary aluminium consumption from year 2011 to 2013 taken from website of European Aluminium Association (EAA). The figure shows that the world's consumption of aluminium alone was 50.2 million tonnes in 2013. China was registered as the main user of primary aluminium worldwide, with 23.2 million tonnes in 2013. Second was Europe with 7.2 million tonnes and North America with 5.5 million tonnes. These major players continue to be the key members for the consumption of primary aluminium.



Source: EAA for Europe, CRU for other regions

Figure 2.1: Aluminium consumption world wide

Aluminium plays a crucial life in human's everyday life. This is because its material properties such as lightweight combined with high strength and resistance to corrosion contribute to high dependency for humans. After iron, aluminium is now the second most

widely used metal in the world [24]. The main reason for aluminium to be in this position are:

- Low weight- aluminium weighs less by volume than most other metals. In fact, it is about one-third the weight of iron, steel, copper or brass. This makes it easier to handle and less expensive to ship.
- High strength- aluminium profiles can be made strong as needed for most applications. Cold-weather applications are particularly well served by aluminium because, as temperature fall, aluminium actually becomes stronger.
- Superior malleability- aluminium combines strength with flexibility and can flex under loads or spring back from the shock of impact.
- Easy machining- aluminium can be finished with a variety of common techniques, including liquid paint, powder coatings, anodizing or electroplating.
- Excellent corrosion resistance- aluminium does not rust. It is protected by its own naturally occurring oxide film, a protection that can be further enhanced by anodizing or other finishing techniques.
- Non-toxic
- Best heat conductor- based on weight and overall cost, aluminium conducts heat and cold better than other metals. These factors make it ideal for applications requiring heat exchangers.
- Non-sparking- aluminium does not emit sparks. This makes it a great choice in applications that involve explosive materials or that are used in highly flammable environments.
- High electrical conductivity- bulk power transmission generally takes place via aluminium because, pound for pound, aluminium is twice as conductive as copper.
- Non-magnetic- because aluminium does not acquire a magnetic charge, it is very useful for high-voltage application, as well as for electronics, especially where magnetic fields come into play or where sensitive magnetic devices are employed.
- Reflective- highly reflective aluminium can be used to shield products or areas from light, radio waves or infrared radiation.

- Non-combustible- aluminium does not burn and even at high temperatures, it does not produce toxic fumes
- Seamless- with aluminium, complex shapes can be realized in one-piece extruded sections without having to use mechanical joining methods. This makes the parts stronger and less likely to leak or loose over time.

CHAPTER 3

METHODOLOGY

3.1 Research Flow Chart

Figure 3.1 illustrates the process flow chart for the project. The project started with discussion and clarification of the title from the supervisor. Identification of research background, problem statement, objective and scope are the second step of this research. Weekly appointments with supervisor also have been agreed and the meetings are conducted accordingly. Literature review started from finding books and journals that are related to the title as a reference of study. From literature review, the way forward on how to conduct the project and experiments in relation to the project was decided. Next step was the preparation of the “dog bone” specimen itself. The specimen was manufactured using the Electron Discharge Machine (EDM). After setting up the optical measurement, the experimental set-up was complete and the experiment was conducted. Once the experiments were done and the video recorded, the snapshots of the video were analyzed using Matlab’s Image Processing Toolbox function to measure the strain data. The experiment was repeated a couple of time to get the best result to validate the optical measurement method. The research ended with documentation and viva.

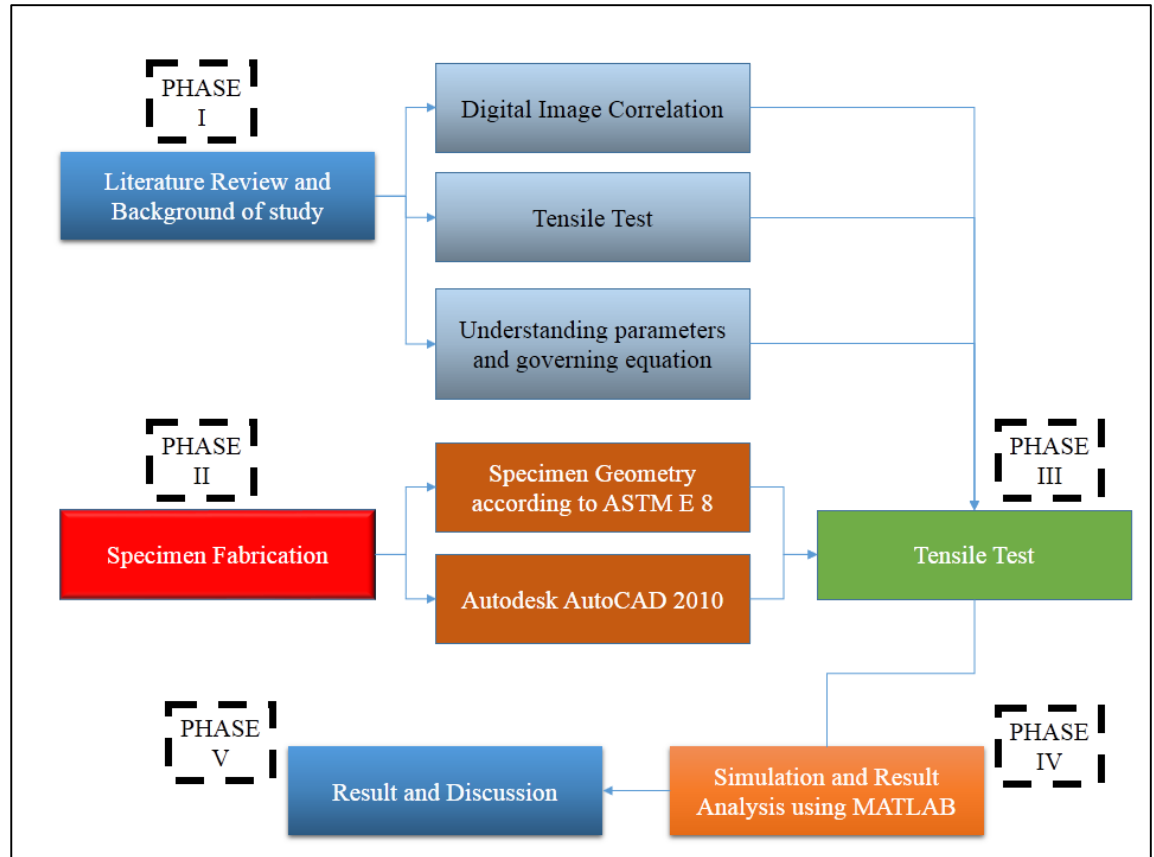


Figure 3.1: Process flow chart of study

Figure 3.2 below shows the procedure and detailed information of the steps.

Define Problem and Component Used

Identification of the problem statement is done by taking into accounts several current issues related to the extent of worldwide scope. Based on those issues, the problem statement, primary objectives are listed down to verify the desired end product of the project. This was followed by the establishment of the scope of the project.

Literature Review

Further studies and research on the subject are conducted to not only gather important details of the project, but also to identify the status of the project through other’s research and studies or any current breakthrough.

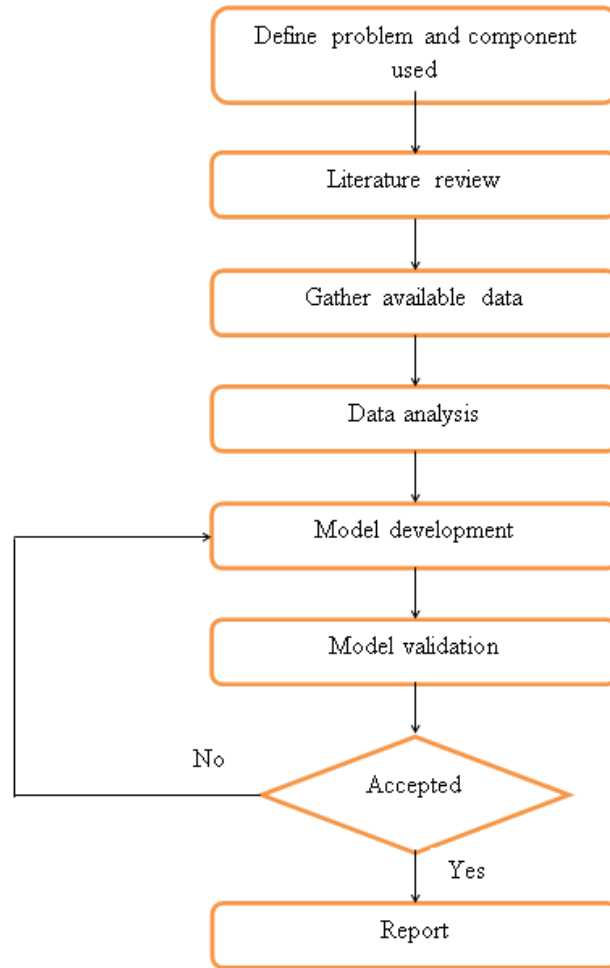


Figure 3.2: Final Year Project Flow Chart

Gather Available Data

Available information or data was collected through the media in order to produce a benchmark prior to the development of the proposed project. The collected data would not only provide a guideline or reality check on the developed project, but it also produces an idea of the expected result of the project. Data to be collected would include Digital Image Processing results and details as well as published results.

Data Analysis

The collected data would be analyzed to identify crucial details required while developing the concept of the design. Other than that, it would also serve as a medium to validate the feasibility and functionality of the proposed design based on the extended studies.

Model Development

The concept generation of the design shall come first in the form of draft followed by concept evaluation to identify the best concept design to be carried onwards. The development of the concept would include simulation based on actual product and variables, generating the detailed design including dimensions and material properties as well as prototype production.

Model Validation

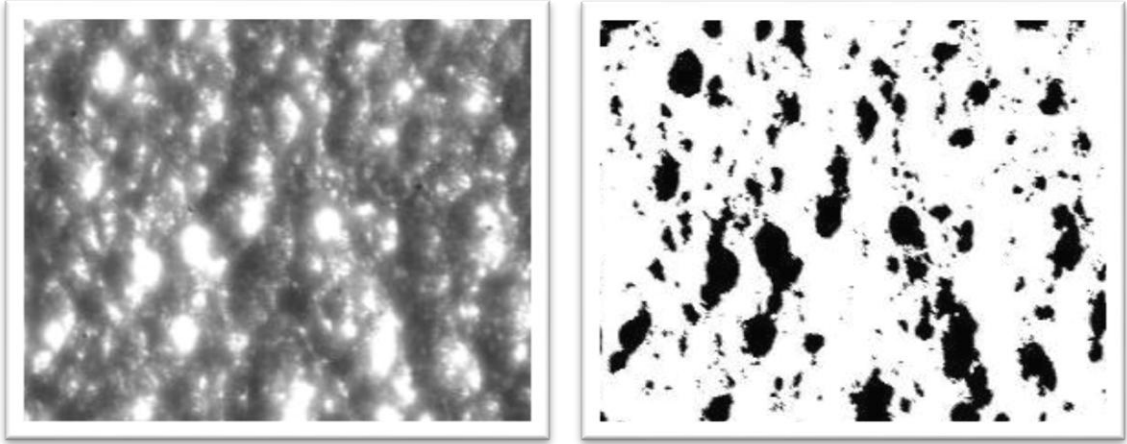
The product shall be validated through a series of experimental measures either within smaller scale or the actual condition. This process is to ensure the product is working well within specified requirements and achieving the expected result. Failure on this stage may require redeveloping of the model again.

Report

Documentations shall be done to record all the information and activities from the initial steps of the proposed project. The purpose of the report would be to serve as a formal and comprehensive set of proof on the development of the proposed project.

3.2 The application of Geometric Approach equation

In 1989, Hovis developed an algorithm known as Centroidal Tracking algorithm which performed the two dimensional full-field deformation measurements by tracking the displacement of the speckle's centroid [20]. Before the analyzing process was carried out, image processing such as filtering and edge enhancement were performed to enhance the surface features such as shown in the Figure 3.3.



(a)

(b)

Figure 3.3: Gray Scale Images from Hovis, 1989 (a) Before surface enhancement

(b) After surface enhancement

Based on Figure 3.3, the position of the speckles centroid were determined and the centroid coordinates, X_c and Y_c computed using the equation expressed as

$$X_c = \frac{\sum[x_i \Delta a_i]}{A} \quad (1a)$$

$$Y_c = \frac{\sum[y_i \Delta a_i]}{A} \quad (1b)$$

$$A = \sum[\Delta a_i] \quad (1c)$$

where x_i and y_i are the pixel coordinates of the speckles, Δa_i is the pixel area where the value is equal to 1, A is the sum of the number of pixels in the total area. After obtaining the centroid coordinates, the change of the interested speckles in the distance between the two subsequent images was determined as shown in Figure 3.4.

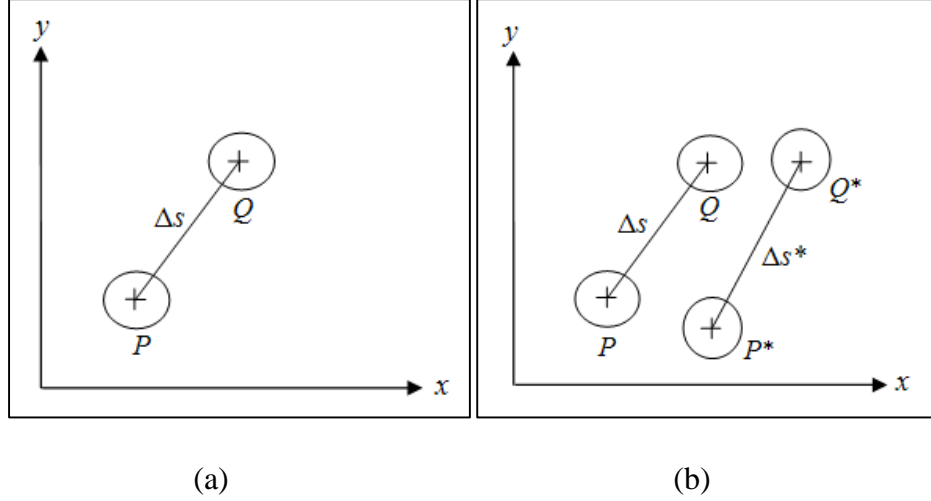


Figure 3.4: The speckles coordinates in an image (a) Before deformation

(b) Before and after deformation

As shown in Figure 3.4, point P and Q were displaced to point P^* and Q^* after the strain inducing event took place. As a result, the relative change in distance, ε_{PQ} between point P and Q was determined by

$$\varepsilon_{PQ} = \frac{\Delta s^* - \Delta s}{\Delta s} \quad (2)$$

where Δs is the length of PQ and Δs^* is the length of P^*Q^* . Hovis suggested that the relative elongation of point P in the direction of Q , ε_{PQ} can be expanded in terms of the strain components ε_{ij} and the strain components were then determined using the Geometric Approach equation as shown below

$$\begin{aligned} & \frac{1}{2} \varepsilon_{PQ}^2 + \varepsilon_{PQ} \\ &= \varepsilon_{xx} \cos^2 \theta_x + \varepsilon_{yy} \cos^2 \theta_y + \varepsilon_{zz} \cos^2 \theta_z \\ &+ 2\varepsilon_{xy} \cos \theta_x \cos \theta_y + 2\varepsilon_{xz} \cos \theta_x \cos \theta_z + 2\varepsilon_{yz} \cos \theta_y \cos \theta_z \end{aligned} \quad (3)$$

where ε_{xx} , ε_{yy} and ε_{zz} are the normal strains in x , y and z -axis respectively ε_{xy} , ε_{xz} and ε_{yz} are the shear strain in xy , xz and yz -plane respectively θ_x , θ_y , and θ_z are

the orientation of the line element PQ in the reference or underformed image as shown in Figure 3.5.

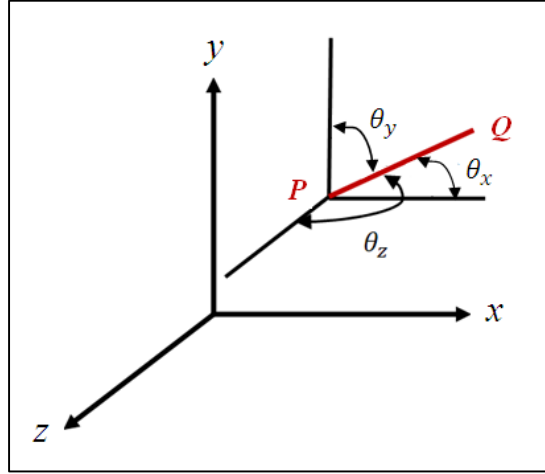


Figure 3.5: The orientation of the line element PQ in the reference image

The orientations of the line element PQ in the reference image were calculated using the equations given by

$$\cos \theta_x = \frac{\Delta x}{\Delta s} \quad (4a)$$

$$\cos \theta_y = \frac{\Delta y}{\Delta s} \quad (4b)$$

$$\cos \theta_z = \frac{\Delta z}{\Delta s} \quad (4c)$$

where Δx , Δy and Δz are the distance between point P and point Q in x , y and z directions respectively in the reference image, Δs is the length of PQ . However, for the surface measurements, the Geometric Approach equation is reduced to two-dimension and the Geometric Approach equation is expressed in the form of

$$\frac{1}{2} \varepsilon_{PQ}^2 + \varepsilon_{PQ} = \varepsilon_{xx} \cos^2 \theta_x + \varepsilon_{yy} \cos^2 \theta_y + 2\varepsilon_{xy} \cos \theta_x \cos \theta_y \quad (5)$$

Based on equation above, a minimum of four points were selected within the reference and the deformed image in order to calculate the strain components, ε_{xx} , ε_{yy} and ε_{xy} . It was reported in Hovis's finding that the accuracy of the results

was increased by selecting more than four points. This Geometric Approach is simple to use and yet precise enough.

3.3 Preparation of Samples and Experimental Set-Up

In order to apply the optical measurement method, tensile tests were conducted by using the Universal Testing Machine and a series of images were captured simultaneously during the strain inducing event. For the experiment, 15 samples of aluminium dog bone specimen were fabricated. Aluminium was selected as the material for the metallic sample since it is easily available in the market. The material properties of aluminium are as in Table 3.1.

Table 3.1: Material properties of aluminium

Parameters	Aluminium
Width(x-axis)	12.5 mm
Length (y-axis)	50 mm
Thickness (z-axis)	3 mm
Modulus of Elasticity, E (Young Modulus)	69 GPa
Ultimate Tensile Strength, S_u	$110 \times 10^6 \text{ N/m}^2$
Yield strength, Y_s	$95 \times 10^6 \text{ N/m}^2$
Poisson's Ratio	0.334

All samples used were deposited with 4 speckles of black paint to create the speckles needed on the specimen.

3.3.1 “Dog Bone Specimen”

In this study, the tensile test for the aluminium samples were conducted in accordance to ASTM E8. By referring to the ASTM standard, the acquired aluminium flat bars plates were cut by the Electrical Discharge Machining (EDM) machine (in Figure 3.6 and Figure 3.7 below) according to the shape and measure shown in Figure 3.8 and Figure 3.9. Table 3.2 shows the dimension of the dog-bone shape specimen used in the tensile test. The Figure 3.9 was drawn using AutoCAD 2010 software.



Figure 3.6: Electrical Discharge Machine



Figure 3.7: The cutting process of the EDM machine

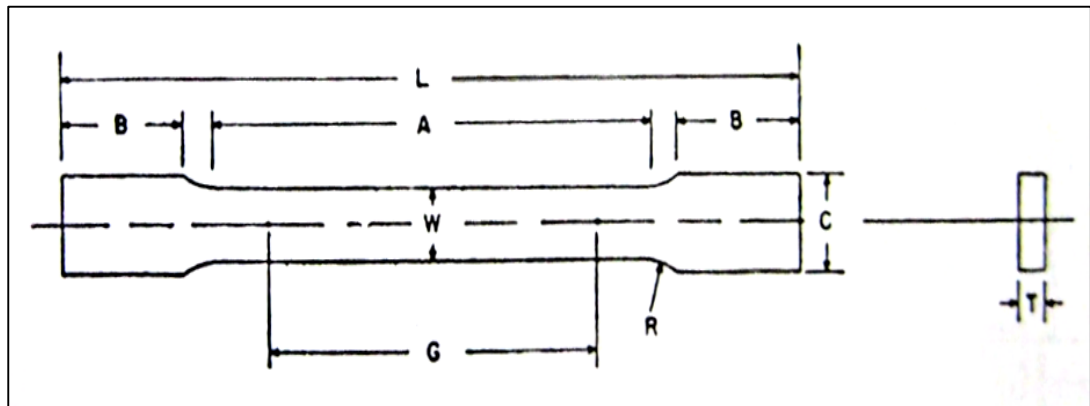


Figure 3.8: The shape of the aluminium specimen

Table 3.2: Dimension of the aluminium specimen

Parameters	Dimensions
G- Gauge Length	50 mm
W- Width	12.5 mm
T- Thickness	3 mm
R-Radius of fillet	53 mm
L-Overall Length	200 mm
A-Length of reduced Section	57 mm
B- Length of grip section	50 mm
C-Width of grip section	20 mm

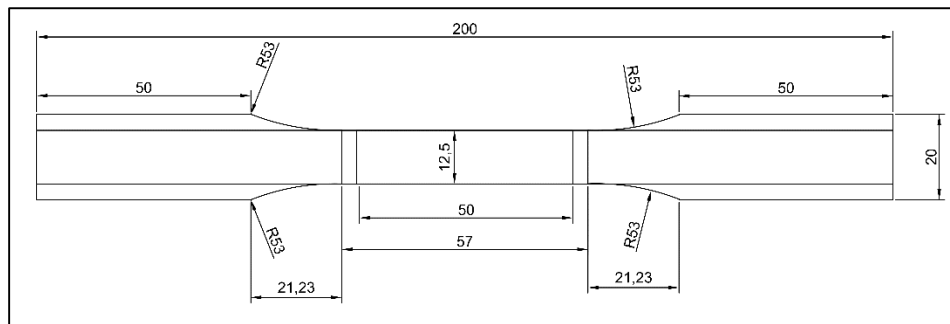


Figure 3.9: The AutoCAD drawing of the dog bone specimen

3.3.2 Experimental Set-Up

For the tensile test in this study, the Universal Testing Machine (UTM) was used to apply load onto the specimen as shown in Figure 3.10.



Figure 3.10: The 20kN UTM machine that was used for the tensile test

At the same time, a consumer version of high-definition video camera was used to record the videos. In this setup, the light sources were unnecessary as it induced too much reflection by the shiny surface of aluminium which caused the camera to be unable to capture precise data. The setup of the experiment is as shown in Figure 3.11 below.



Figure 3.11: The equipment used in the tensile test

Before the tensile test was started, it was necessary to make sure that the video camera was properly installed on top of the tripod. Since the tripod can be rotated in yaw, pitch and roll axis, a series of alignment checking were carried out to ensure that the video camera was installed correctly. A spirit level was placed on the body of the video camera and the alignments were adjusted to be flat in the axis of pitch and roll. Besides this, the specimen was vertically aligned too during the installation of the specimen into the middle of the UTM grippers. The spirit level was placed alongside the dog-bone shape specimen and the alignment of the specimen in the vertical axis was verified.

After the alignments checking were done in the experimental set-up, all the equipment such as the UTM grippers, the tripod, the video camera were kept untouched for the entire tensile test. Furthermore, the experimental set-up discussed above is very suitable for aluminium specimen.

3.3.3 Tensile Test Experiment and Video Recording during Strain Inducing Event

In accordance to ASTM E8, 5 specimen were tested using the UTM. At the beginning of the tensile test, the specimens were carefully installed into the UTM grippers as shown in Figure 3.12. Next, the extensometer was gently mounted on the specimen and the results obtained served as a benchmark for values determined from the optical strain measurement method.

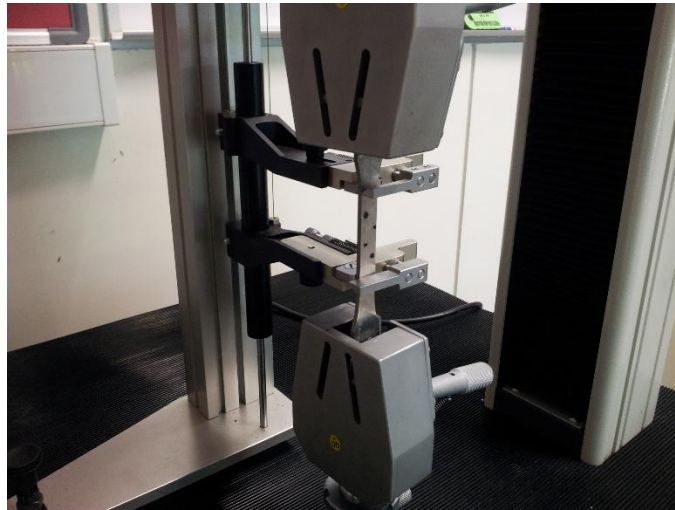


Figure 3.12: The setting of the specimen before the experiment being conducted

After this, the UTM was switched on and the cross head speed was set to the rate of 0.01 mm/s. Meanwhile, the video camera were adjusted according to the setting for aluminium as in Table 3.3 below.

Table 3.3: Settings for the video camera

Settings	Aluminium
Aperture	F2.0
Frame Rate	25 fps
Image resolution	1920x1080

The tensile test was conducted once the specimen and the extensometer were properly installed. Simultaneously, the videos were recorded using a consumer version of high-

definition video camera at the rate of 25 fps. The videos recording continued until the material split to make sure all data was captured by the video camera as shown in Figure 3.13.

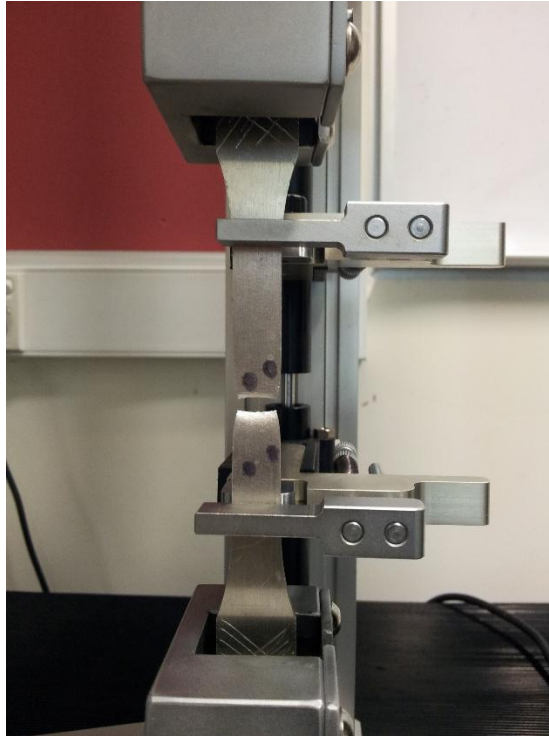


Figure 3.13: The end resultant image of the aluminium specimen.

3.4 Optical Strain Measurement Method Validation with Experimental Results

First, the elongation values determined by the extensometer were extracted from the data logger of Universal Testing Machine (UTM). By using the elongation values, the strain values were then calculated and the obtained results served as a benchmark for values determined by the optical strain measurement method. Based on the data shown in Figure 3.14, the stresses experienced by the specimen during the tensile test were determined and the modulus of elasticity of the specimen was then obtained by utilizing the stress strain relationship.

Time:sec	Load:kgf	Load:N	Stroke:mm
0	1	9.80665	0
0.1	1.128	11.0619012	0.00382
0.2	1.145	11.22861425	0.00483
0.3	1.153	11.30706745	0.01571
0.405	1.772	17.3773838	0.2255
0.51	10.077	98.82161205	0.54903
0.61	38.062	373.2607123	0.88314
0.715	84.337	827.0634411	1.15128
0.815	129.715	1272.069605	1.24658

Figure: 3.14 Elongation values extracted from the data logger

Meanwhile for the experimental results, the recorded videos were 1st processed using the video camera before they were transferred to the computer. The MATLAB program was designed to execute two images that are acquired at two different states. By selecting one image before deformation and the other one after deformation, a series of images were extracted from the recorded videos. By using the built-in function in the video camera, Capturing Photos from Video, a series of images with the image resolution 1920x1080 pixels were captured from the recorded videos. These extracted images were then processed by using the MATLAB program and the two dimensional deformation measurement such as the normal strain in the x and y axis and the shear strain were determined. From the determined values, only the normal strain was selected and compared with the benchmark values as the extensometer only provides the normal strain values in y direction.

3.5 Gantt Chart and Key Milestones

Table 3.4 is the representation of the activities that have been done in the research methodology to complete strain determination using the digital image correlation technique. The chart includes the time frame for Final Year Project 1 and Final Year Project 2 together with the key milestones which have been accomplished.

Table 3.4: Gantt Chart and Key Milestones for FYP I and FYP II

Item/Week	FYP I														FYP II													
	1	2	3	4	5	6	7	8	9	10	11	12	13	14	1	2	3	4	5	6	7	8	9	10	11	12	13	14
Selection of FYP Topic	█	█																										
Background Study & Literature Review		█	█	█	█	█																						
Familiarization of ASTM E 8 standards			█	█	█	█	█																					
MATLAB programming							█	█	█	█	█	█																
Fabrication of Specimen									█	█	█	█	█	█														
Tensile Testing															█	█	█	█	█	█	█	█						
Data Evaluation and Analysis																					█	█	█	█	█	█	█	█
Presentation and Thesis Report																										█	█	█

3.6 Tools required

The software used in this research experiment were AutoCAD 2010, Matlab R2009a and Matlab R2009b. AutoCAD 2010 is a software application that is capable of high resolution drafting with high accuracy. In both revisions of Matlab, the Image Processing Toolbox was used because it provided a set of reference-standard algorithms, functions and applications for image processing. Besides that, some heavy industry grade machines were also used extensively in

this research. The machines were Universal Testing Machine and Electrical Discharge Machining (EDM) machine. The EDM machine is a manufacturing machine whereby the “dog bone” specimen was produced using electrical discharges. The machine removes work piece by a series of rapidly recurring current discharges between two electrodes, separated by a dielectric liquid and subject to electric voltage. The video camera used was the Canon LEGRIA HF S10 - HD Camcorder, 8.0MP Canon HD Camera System, 64GB Dual Flash Memory, Manual control options and 8MP photos (HFS10).

CHAPTER 4

RESULTS AND DISCUSSION

4.1 Validation of Optical Strain Measurement Method with Experimental Results

The tensile test of 5 main specimens was carried out after many test runs to determine the light concentration, the camera best spots and also the test speed. Even though the recommended speed for aluminium was 0.02 mm/sec by the ASTM E8 standards, the test speed was ultimately too fast to capture in detail every moment of the tensile test. At the end, a test speed of 0.001 mm/sec was decided. One experiment took an average of 6 to 8 minutes which resulted to 40 to 50 images taken at distinctive time intervals for the measurement of strain using Matlab. The experiment was run concurrently with an extensometer to validate the results of the Matlab. Table 4.1 below shows the results obtained from the extensometer from the extensometer for the experiments conducted.

Table 4.1: Results obtained from the extensometer for the tensile test experiments

Test No.	Width, mm	Thickness, mm	Area, mm ²	Max Load, kN	Tensile Strength, kgf	Yield Strength (U), Mpa
1	12.50	3.0	37.50	4.083	417.8	107.2
2	12.50	3.0	37.50	4.082	416.2	107.7
3	12.50	3.0	37.50	4.099	418.0	107.2
4	12.50	3.0	37.50	4.113	419.4	108.4
5	12.50	3.0	37.50	4.084	416.4	107.7
Average	12.50	3.0	37.50	4.095	417.5	107.8
SD ^(N-1)	0.00	0.0	0.00	0.014	1.5	0.5

Figure 4.1 shows the 5 tensile test results which were automatically plotted by the software that links the extensometer with the UTM machine.

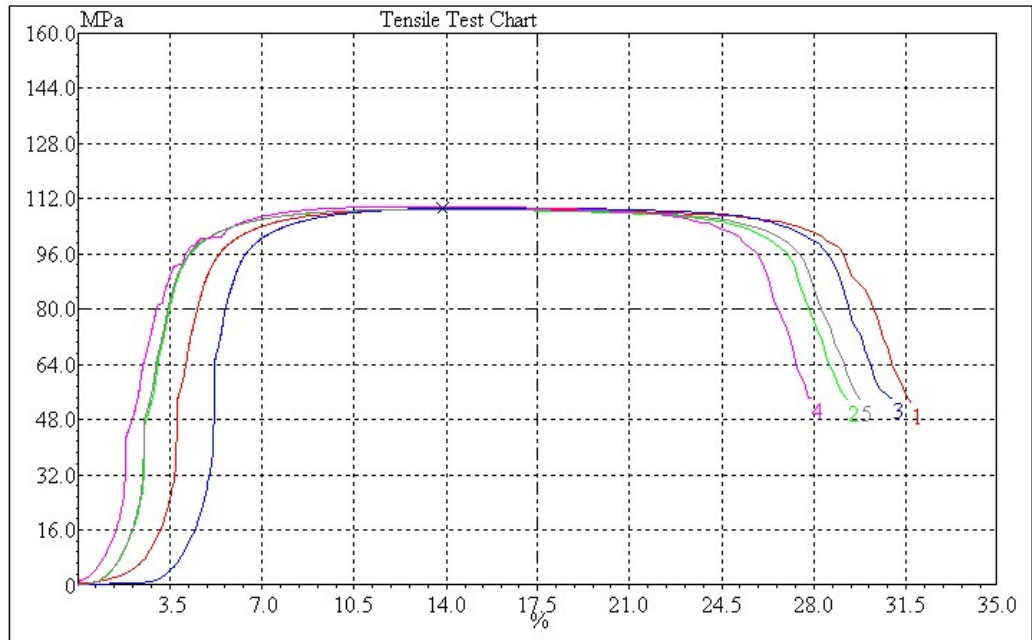


Figure 4.1: The tensile test chart

In order to apply the Matlab program, tensile tests were conducted and the results determined by the optical measurement method were validated with the benchmark values obtained through extensometer. By using the UTM, the aluminium specimens were tested. At the same time, videos were recorded at the strain inducing event using the high-definition video camera. These videos were captured continuously until fracture.

By extracting the values from the UTM's data logger, a series of calculations were performed in Microsoft Excel spreadsheet. At the same time, the extracted images from the recorded videos were then analyzed using the Matlab program and the 2D deformation measurement were determined. All the necessary information of the tensile tests were recorded and used for the calculation of important properties. The stress and the strain experienced by the specimen at the specific time interval were calculated and the modulus of elasticity for each specimen was determined which will be further explained in the next segment in the report. In addition, the results

determined by the extensometer and the optical strain measurement method were compared to each other and the deviations between the two was obtained.

By using the strain values determined by the extensometer, the stress-strain curves were plotted for the aluminium specimens respectively. Overall, the shape of the plotted stress strain curve, as shown in Figure 4.2, was found to be exactly the same as the shape of the load-elongation curves generated by UTM's data logger. This was because the stress and the strain of a specimen is determined by dividing the load and the elongation with the constant factors.

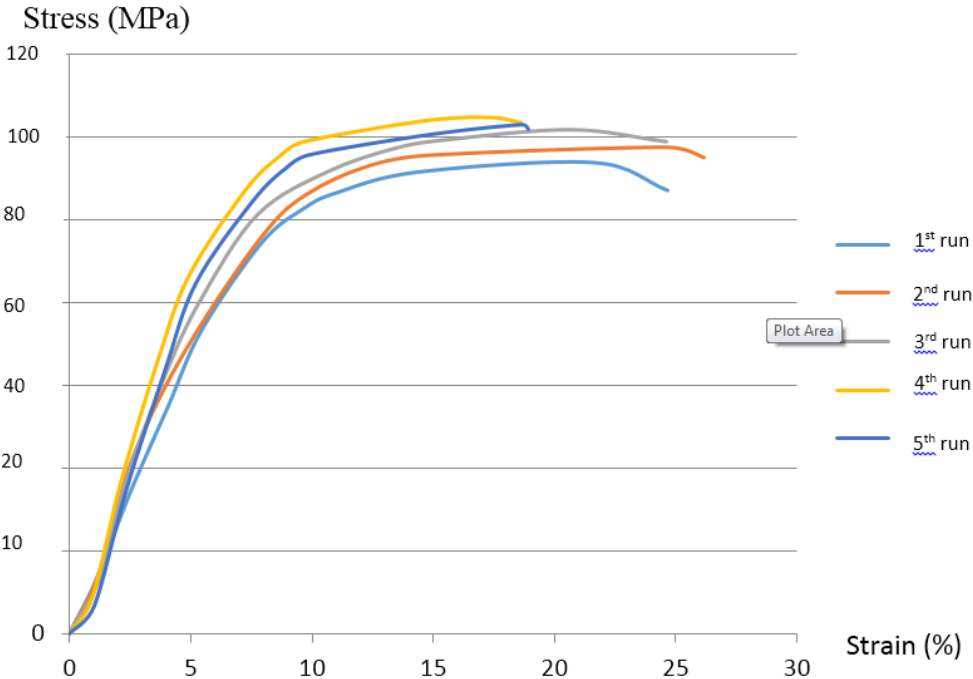


Figure 4.2: Stress strain curve for all five aluminium specimens

Besides, the trend for the stress-strain curve determined from the extensometer reading and the optical strain measurement method were similar and fitted together perfectly. However, some deviations were still observed at the beginning of the elastic region in the stress strain curve. By analyzing the results determined by the optical strain measurement method, the position of the selected speckles in the 1st few pairs of images were barely displaced. Even though the images have the image

resolution of 34.4 pixels/mm and 33.05 pixels/mm in the x and y directions respectively, the captured images were unable to record the very small displacement accurately. Figure 4.3 until Figure 4.13 shows the images that were used in the Matlab programming to calculate the strain. Figure 4.12 shows the best illustration when necking could be seen on the specimen. The rupture also occurs in the area of the four speckles. From all the other images taken at different time interval are inserted into Matlab to calculate their strain value.

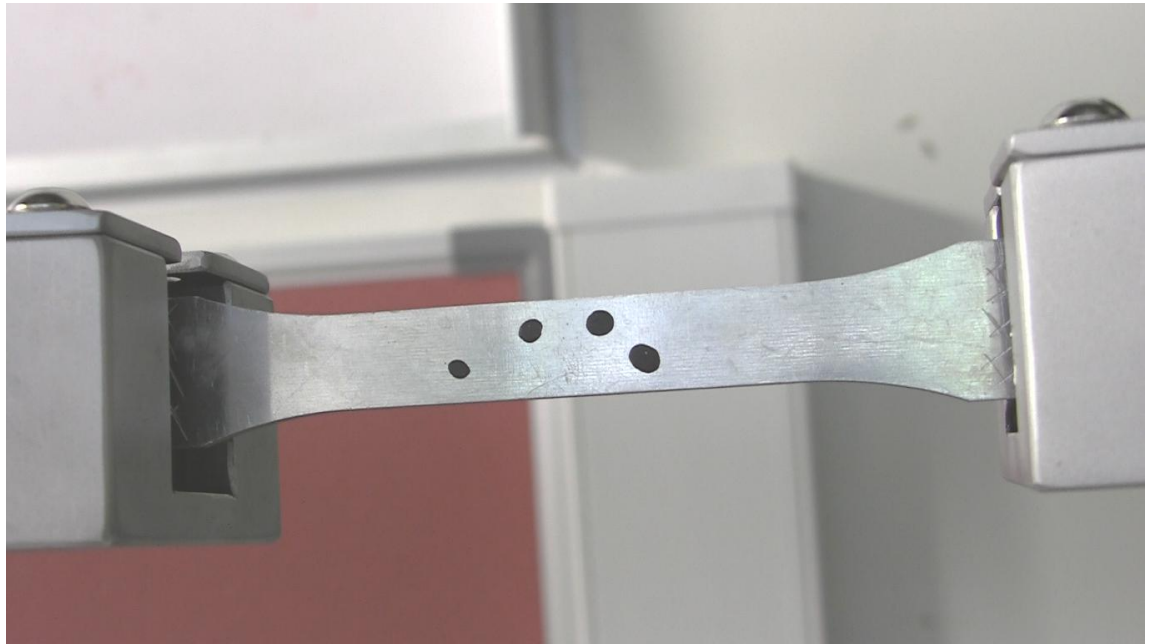


Figure 4.3: Specimen image taken at 1 second

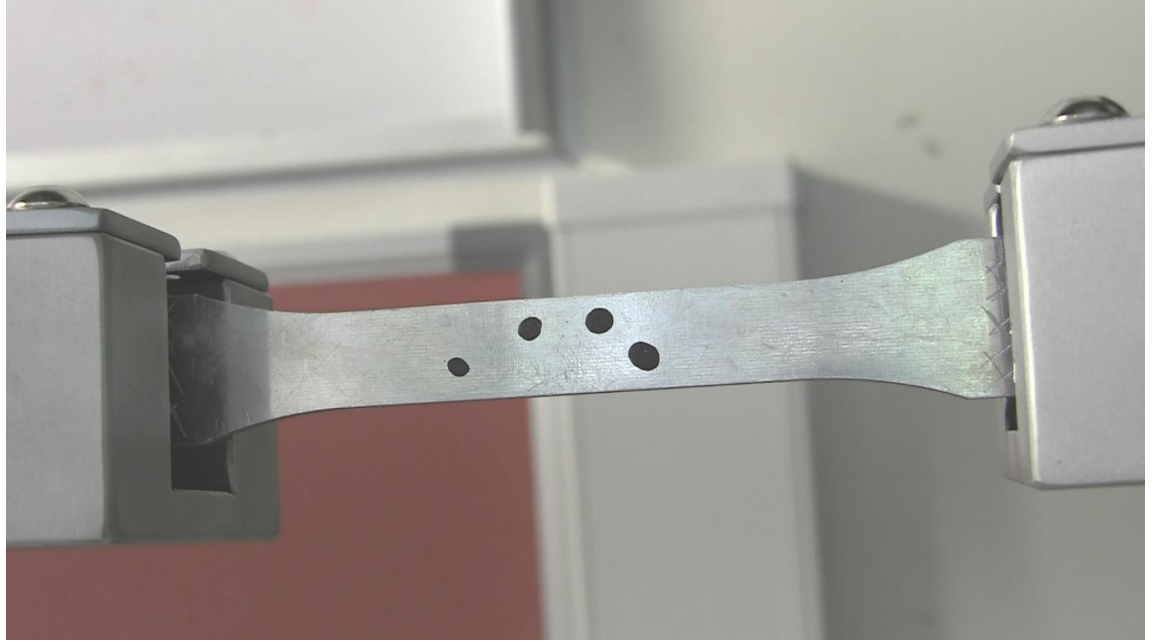


Figure 4.4: Specimen image taken at 44 seconds

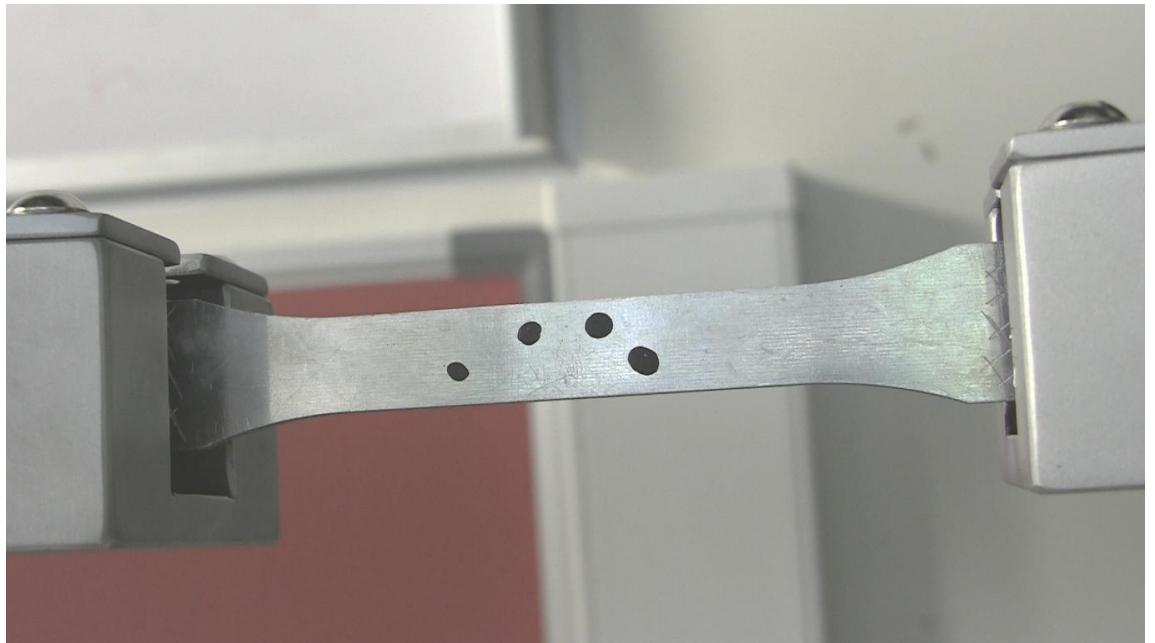


Figure 4.5: Specimen image taken at 90 seconds

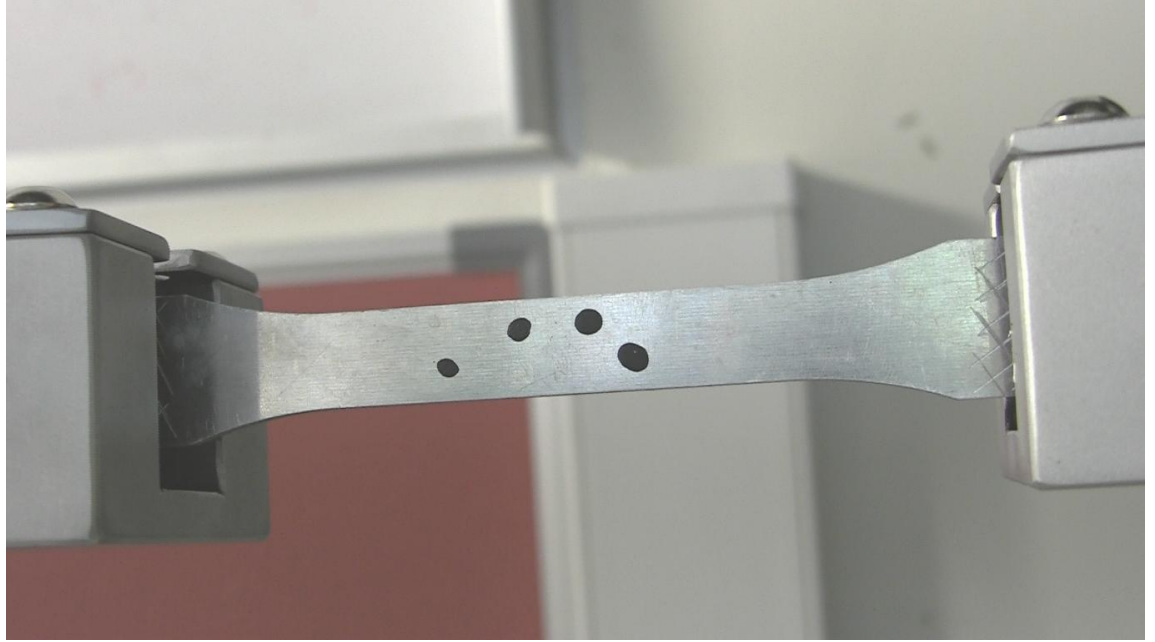


Figure 4.6: Specimen image taken at 134 seconds

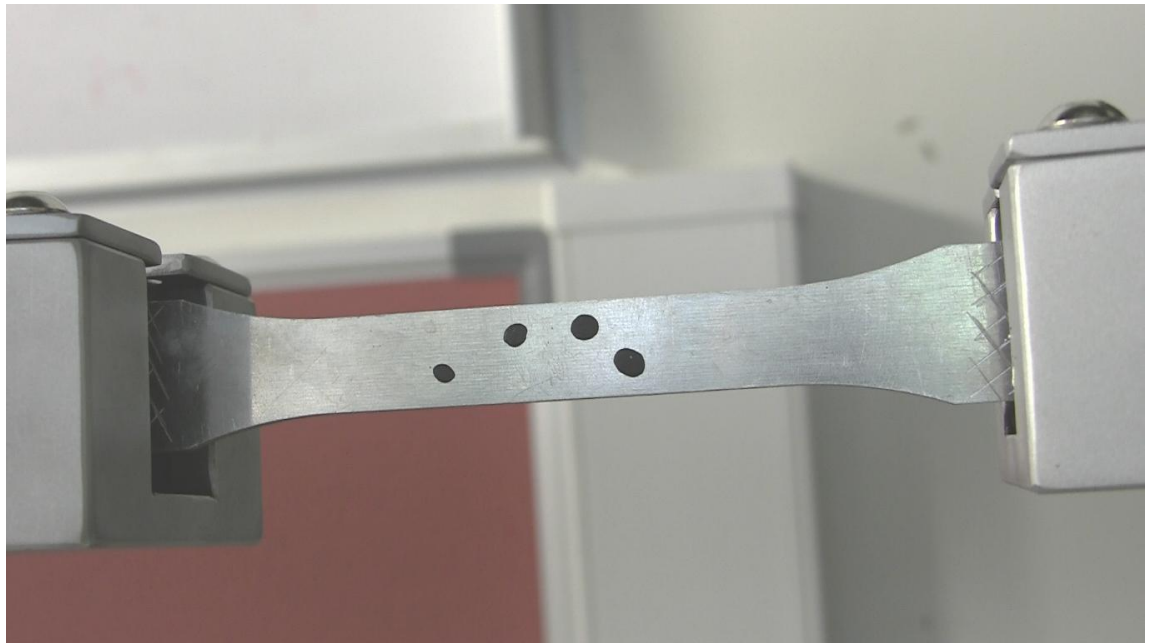


Figure 4.7: Specimen image taken at 178 seconds



Figure 4.8: Specimen image taken at 222 seconds



Figure 4.9: Specimen image taken at 266 seconds

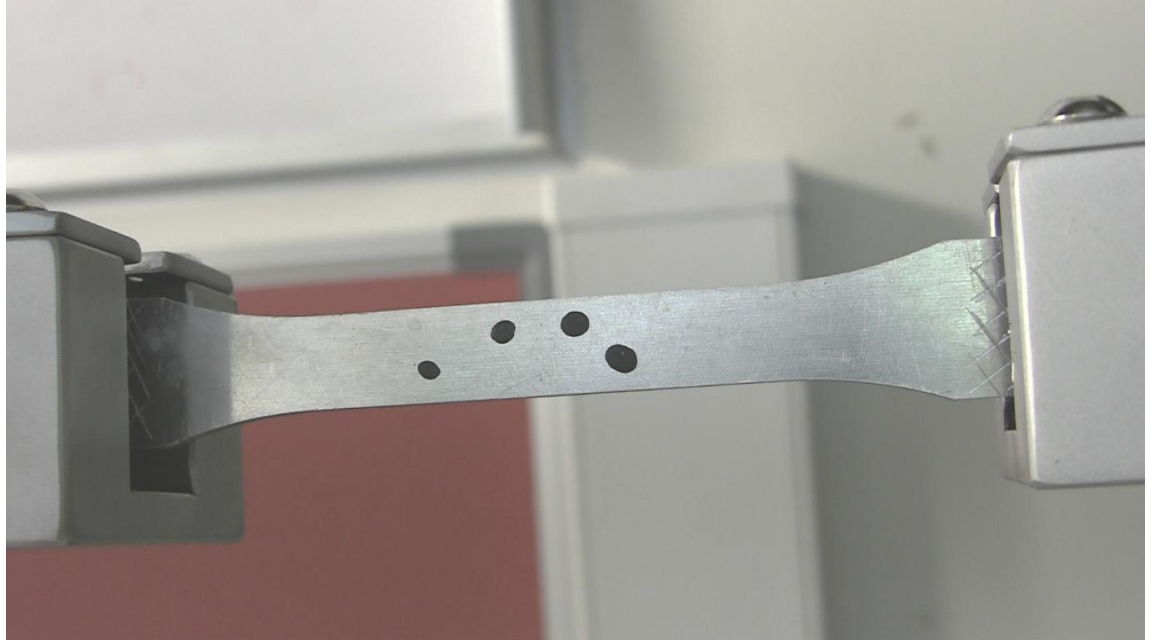


Figure 4.10: Specimen image taken at 310 seconds

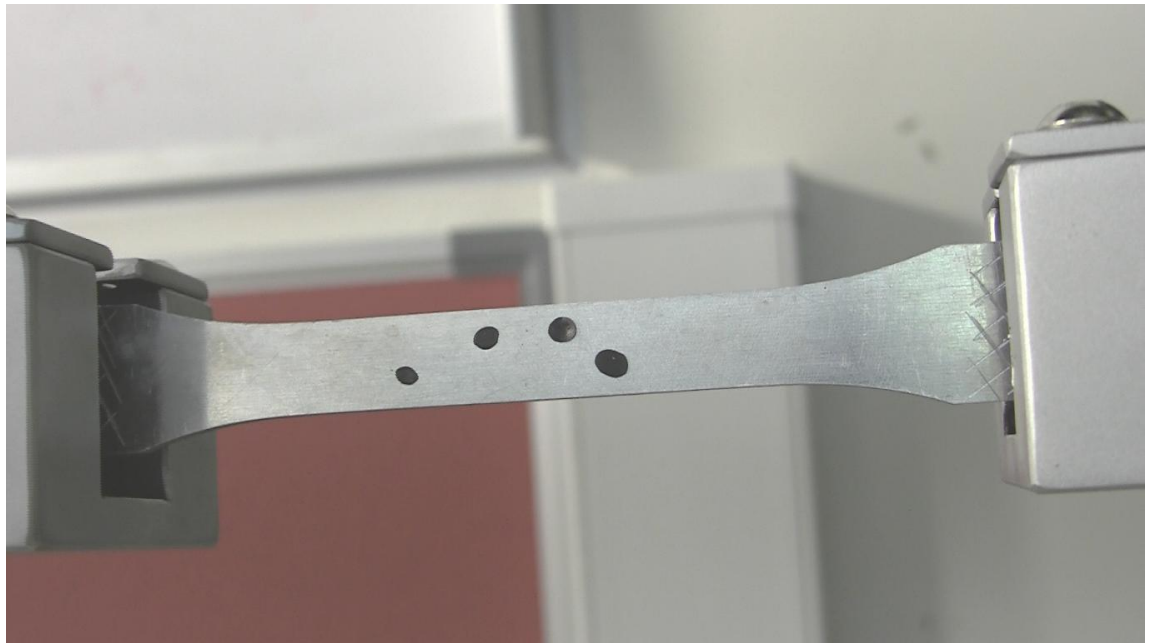


Figure 4.11: Specimen image taken at 354 seconds

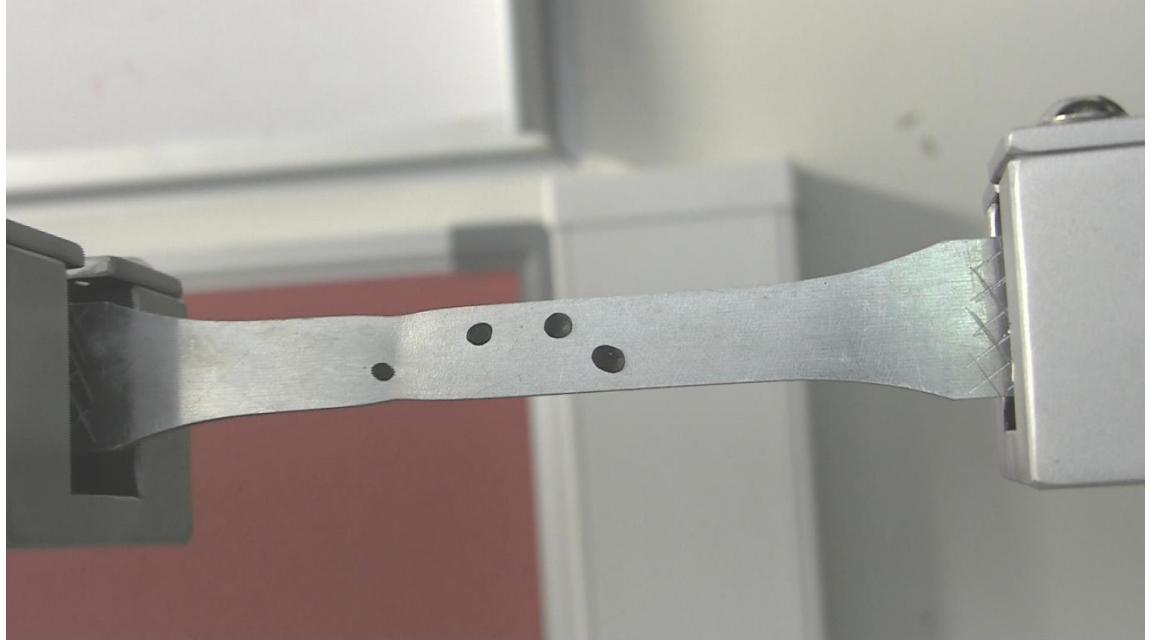


Figure 4.12: Specimen image taken at 398 seconds

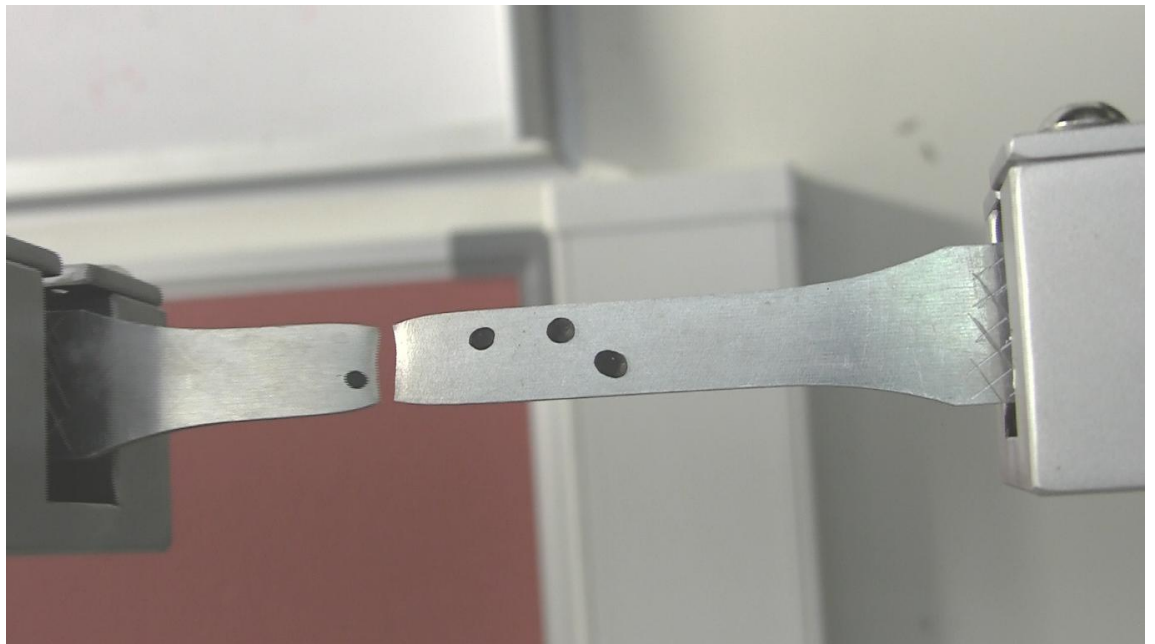


Figure 4.13: Specimen image taken at 482 seconds

From the comparison of results determined by the extensometer and the optical strain measurement method, the small deviations proved that the optical strain measurement method was capable to determine the strain values correctly.

4.2 Comparison to Specimens Material Properties

For the comparison of the specimens' material properties, the modulus of elasticity of the aluminium was determined by analyzing the stress-strain curves within the elastic regions in Figure 4.14. By using the results determined by the extensometer and the optical strain measurement method, the gradient of the stress-strain curves for the aluminium were plotted. To find the modulus of elasticity of the aluminium specimens, the gradient of the stress-strain curve for the first specimen was plotted. The strain values determined from the extensometer readings served as the benchmark for the strain values determined by the optical strain measurement method. Meanwhile, two straight lines which best fitted the dotted points were plotted. As a result, the modulus of elasticity of the aluminium specimen was successfully determined by the two methods mentioned above.

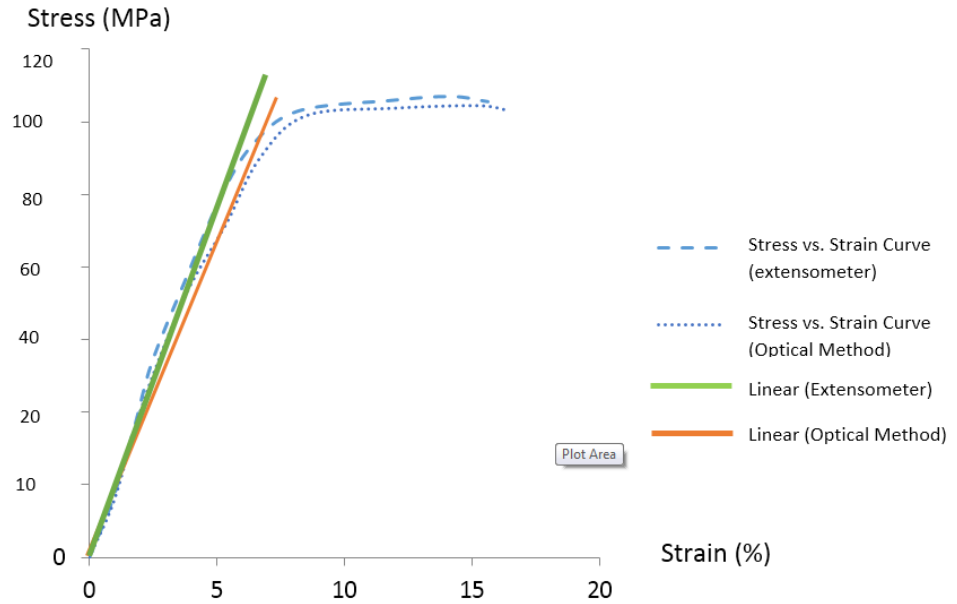


Figure 4.14: Determination of the modulus of elasticity for the specimen

The modulus of elasticity for the aluminium specimen determined by the extensometer and the optical strain measurement method were found to be 91 GPa and 85 GPa, respectively. Based on these results, the first aluminium specimen was 6.59% off the benchmark value. Meanwhile, Table 4.2 shows the comparison of the modulus of elasticity determined by the extensometer and the optical strain measurement method for all five specimens that have been tested in the tensile test. Based on Table 4.2, the average value of the modulus of elasticity determined by the extensometer was 92.2 GPa. While for the average value of the modulus of elasticity determined by the optical strain measurement method was found to be 85.5 GPa. As a result, the average deviation was found to be 6.99% off the benchmark value. Through the comparison of the modulus of elasticity determined by the two methods mentioned above, the optical strain measurement method had been verified and a good agreement was achieved as the deviations were found to be around 7% off the benchmark value.

Table 4.4: Comparison of the modulus of elasticity determined by the extensometer and the optical strain measurement method

Specimens	Extensometer	Optical Strain Measurement Method	Deviation (%)
1	91 GPa	85 GPa	6.59
2	95 GPa	83 GPa	12.6
3	93 GPa	89 GPa	4.30
4	92 GPa	88 GPa	4.34
5	90 GPa	84 GPa	7.14
Averag	92.2 GPa	85.8 GPa	6.99

The Figure 4.15 to Figure 4.17 shows result, before and after of the tensile test experiments. Figure 4.15 is the zoomed out image of the whole specimen, showing the 4 four speckles which was positioned inside the gauge area of the specimen.



Figure 4.15: Specimen before tensile test

Figure 4.16 shows the detail view of the specimen. The four speckles was placed in irregular pattern for all the 15 specimens. This is to ensure the selection of speckles was made easier during the Matlab simulation process.



Figure 4.16: Four irregular placement of the speckles that will assisted in identification of the speckles during Matlab simulation.

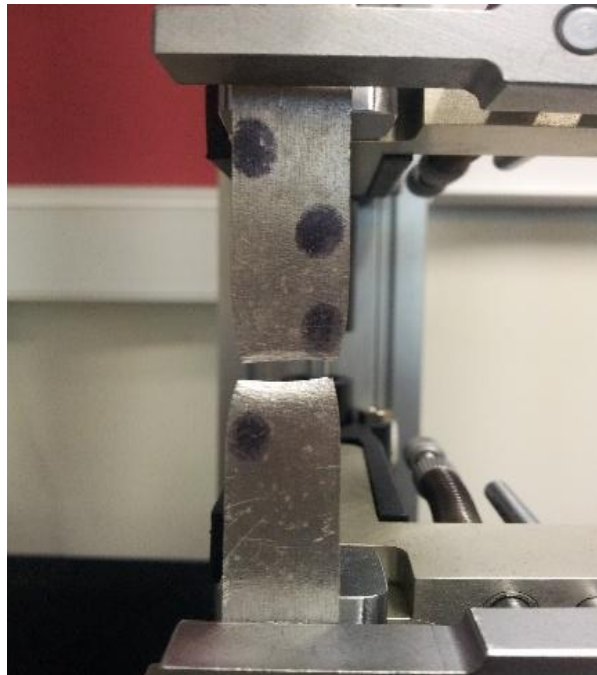


Figure 4.17: Final image at $t=360$ seconds which illustrates the hourglass effect where the localized stress have occurred.

Figure 4.18 shows the difference in length of two different specimens of aluminium. This change in length was calculated to determine the strain of the specimen. Besides that, from visual inspection, the speckles placed in the gauge area of the specimen does provide easier identification of speckles during the Matlab simulation.



Figure 4.18: Specimen on the right is the undeformed specimen while the specimen on the left is the deformed specimen.

CHAPTER 5

CONCLUSIONS AND RECOMMENDATIONS

5.1 Conclusions

A series of tensile tests were also conducted using the Universal Testing Machine. Before the experiments were conducted, the surface of the specimens had been deposited with the black paint to create speckles pattern effect. By adopting the ASTM E8, a total of five specimens made of aluminium materials respectively were tested. During the strain inducing event, the extensometer was used for strain measurement which served as a benchmark for the values determined from the optical strain measurement method. Simultaneously, videos were recorded using a consumer version of high-definition video camera. Then, the extracted images from the recorded videos were analyzed by the MATLAB program and the two-dimensional deformation measurement was successfully determined. In the validation of the optical strain measurement method with the experimental results, the results determined by the extensometer and the optical strain measurement method were compared to each other. By using the strain values determined by the extensometer, the stress-strain curves were plotted and they served as benchmarks for values determined by the optical strain measurement method. For the aluminium specimens, the strain values determined by the two methods mentioned above were close to each other. Although some deviations were still observed during the comparison of the results determined by the extensometer and the optical strain measurement method, the deviations were reasonably small.

In the last part of this study, the modulus of elasticity of the aluminium specimens were determined successfully using the optical strain measurement method. For the aluminium specimens, the modulus of elasticity was found to be 85.5 GPa and 6.59% off the benchmark value. By referring to the comparison of the modulus of elasticity determined by the two methods

mentioned above, the optical strain measurement method had been verified and a good agreement was achieved as the deviations were found to be very small.

By comparing the results determined by the extensometer and the optical strain measurement method, the deviations in terms of percentage had been found to be relatively small. In conclusion, the two-dimensional measurement algorithm that calculates the strain in a loaded structural had been developed successfully and tested in the study. In addition, the consumer version of high-definition video camera has been proven to be capable to capture the deformed images impeccably.

5.2 Recommendation

After completing this study, there are several piece of work which merit further study and the recommendation are given below:-

- 1) To use ANSYS in determining the effect of extensometer on the specimen itself. This is because the analysis of the force that is applied by the extensometer on the testing material itself.
- 2) Installation of hydraulic gripper in the UTM.

REFERENCES

- [1] "DANTEC DYNAMICS," [Online]. Available:
<http://www.dantecdynamics.com/Default.aspx?ID=1030>.
- [2] S. C. L. T. Z.Q. Tue, "Finite Element Modeling of Geomaterials Using Digital Image Processing," China, 2002.
- [3] A. K. a. X. Wang, Photoelasticity in Strain Measurements and Stress Analysis, New Jersey: Prentice Hall, 2001.
- [4] M. E. Vohringer), "Phys Status Solidi B," vol. 19, p. 793, 1967.
- [5] I. Y. S. Y. M. Y. Tsuji N, "Scripta Mater," vol. 47, p. 893, 2002.
- [6] Z. A. Z. M. D. A. Shibkov AA, "Phs Solid State," vol. 53, p. 887, 2011.
- [7] R. Schwab and V. Ruff, "On the nature of the yield poin phenomenon," Elevier Ltd., Germany, 2012.
- [8] Keith E. F. , Mechanical Engineering handbook, Boca Raton: CRC Press LLC, 1999
- [9] R. b. T. R. V. V. a. D. J.-C. Rotinat, "Three Optical Procedures for Local Large-Strain Measurement," *strain, An International Journal for Experimental Mechanics*, vol. 37, no. 3, pp. 89-98, 2001.
- [10] M. A. D. I. Piober G, "Mem l'artillerie," vol. 5, p. 501, 1842.
- [11] Tao G. and Xia Z. , 2007, "A non-contact real time strain measurement and control system for multiaxial cyclic and fatigue tests for polymer materials by digital image correlation method", *Polymer Testing* 24 (2005): 844-855
- [12] S. K. M. R. B. A. L. Khoo Sze Wei, "Development of an Optical Strain Measurement Method Using Digital Image Correlation," *Asian Journal of Scirntific Research*, vol. 6, pp. 411-422, 2013.
- [13] L. E. Han BQ, "Advanced Engineering Material," vol. 7, p. 457, 2005.
- [14] A. C. M. I. J. Gonzalez-Doncel G, "Acta Metall Mater," vol. 43, p. 4281, 1995.
- [15] T. A. u. l. H. P. Gaal I, "Int J Refract MetH," vol. 24, p. 325, 2006.
- [16] M. GA., "Phys Solid State," vol. 47, p. 656, 2005.
- [17] H. EO, Yield Point Phenomena in Metals and Alloys, London: Macmillan, 1970.
- [18] L. W. Dingers, "Polytech J," vol. 155, p. 18, 1860.

- [19] "THE FREE DICTIONARY BY FARLEX," Princeton University, Farlex Inc. , 2003-2013. [Online]. Available: <http://www.thefreedictionary.com/grating>. [Accessed 16 AUGUST 2013].
- [20] "Importance of Yield Strength & Plastic Deformation to Civil Engineers," [Online]. Available: <http://www.leonghuat.com/articles/civil%20engineering.htm>.
- [21] P. L. D. D. E. M. T. Robyn H. pritchard, "Precise Determination of the Poisson ratio in soft materials with 2D digital image correlation," Cambridge, 2013.
- [22] L. X. Zhou Guofeng, "Application of Digital Speckle Correlation Method Combined with Edge Tracking in Sheet Tensile Test," China, 2010.
- [23] "Growth-Dedicated Call-10/1," pp. 1-3.
- [24] M. C. A. L. V. Valle, "Dynamic optical method for local strain measurements: principle and characteristics," *JOURNAL DE PHYSIQUE IV*, vol. 4, no. III, pp. 59-64, 1994.
- [25] Y. W. R. L. Lianxiang Yang, "Advanced Optical Methods for Whole Field Displacement and Strain Measurement," 2011.
- [26] T. K. Hirosuke Inagaki, "Yield Point Elongation in Al-Mg Alloys," *Material Science Forum*, Vols. 331-337, pp. 1303-1308, 2000.
- [27] Wattrisse B, Chrysochoos A., Muracciole J-M and Nemoz-Gailard M., "Analysis of Strain Localization during Tensile Tests by Digital Image Correlation", *Experimental Mechanics*, Vol. 41, No 1